

A Numerical Study on the Effect of Inlet Guide Vane Angle on the Performance of Francis Hydraulic Turbine

Chul-Ho Kim[†]

(Manuscript : Received SEP 15, 2005 ; Revised OCT 27, 2005)

Abstract : The objective of this study is an understanding of the effect of inlet flow angle on the output power performance of a Francis hydraulic turbine. An optimum induced angle at the inlet of the turbine is one of the most important design parameters to have the best performance of the turbine at a given operating condition. In general, rotating speed of the turbine is varied with the change of water mass flowrate in a volute. The induced angle of the inlet water should be properly adjusted to the operating condition to have maximum energy conversion efficiency of the turbine. In this study, a numerical simulation was conducted to have detail understanding of the flow phenomenon in the flow path and output power of the model Francis turbine. The indicated power produced by the model turbine at a given operating condition was found numerically and compared to the brake power of the turbine measured by experiment at KIER. From comparison of two results, turbine efficiency or energy conversion efficiency of the model turbine was estimated. From the study, it was found that the rotating power of the turbine linearly increased with the rotating speed. It means that the higher volume flow rate supplied, the bigger torque on the turbine shaft generated. The maximum brake efficiency of the turbine is around 46% at 35 degree of induced angle. The difference between numerical and experimental output of the model turbine is defined as mechanical efficiency. The maximum mechanical efficiency of the turbine is around 93% at 25~30 degree of induced angle.

Key words : Francis hydraulic turbine, Computational fluid dynamics(CFD), Finite volume method(FVM), Body-fitted coordinate(BFC), Indicated power, Inlet guide vane, Induced angle

1. Introduction

Francis hydraulic turbine is classified

into an impulse-type turbine because it uses pressure and kinetic energy of flowing water to generate the rotating

[†] Corresponding Author(Department of Automotive Engineering, Seoul National University of Technology),
E-mail : hokim@snut.ac.kr Tel : 02)970-6347

power^{[1], [2]}. Especially the impulse-type turbine is adaptable to the place where hydraulic head is low but with high mass flowrate. This research is a preliminary study for the development of design algorithm of Francis hydraulic turbine. For an optimum design of Francis hydraulic turbine, detailed understanding of flow phenomenon in blade-to-blade path and volute of the turbine is very important. An experimental approach for this gives very limited information of flow phenomenon in the control volume. However, a numerical simulation must be very useful tool to have detailed information of the flow field and it makes possible to develop an optimum design algorithm of the hydraulic turbine.

With the change of mass flowrate of water at inlet of the turbine, the induced angle should be adjusted to the proper angle to keep the water flow smooth in the flow path. Otherwise unstable turbulent flow is generated in blade-to-blade path of the turbine and the flow separation occurs on the vane surface. All these complicated turbulent flow changes the useful energy to entropy. Therefore an inlet guide vane system is applied to control the flow induced angle with the change of mass flowrate in the turbine system.

In this study, numerical simulation is conducted to understand the effect of induced angle on the output power performance of a model Francis hydraulic turbine. The result is compared to the experimental output conducted at Korean Institute of Energy Research (KIER)^[6] to estimate energy conversion efficiency, mechanical efficiency and mechanical loss

power of the model turbine. The best operating condition of the model turbine is also found from this research.

2. Fluid flow characteristics and geometry of model turbine

Francis turbine system consists of two main components: inlet guide vanes and rotor. The inlet guide vane directs the inlet water into the rotor with a tangential component of velocity. The inlet angle of water controlled by the guide vanes should be adjusted to the operating conditions: flowrate and head situation, to have optimum performance of the hydraulic turbine. As water passes through the turbine region, the flow changes abruptly its direction to axial and exits into a diffuser which acts to convert the kinetic energy remaining in the water into flow energy.

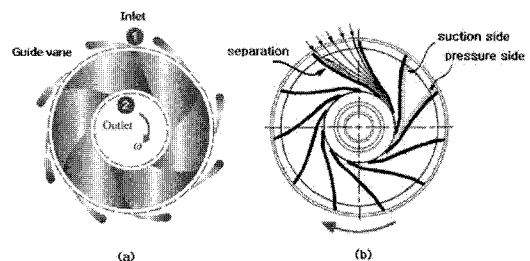
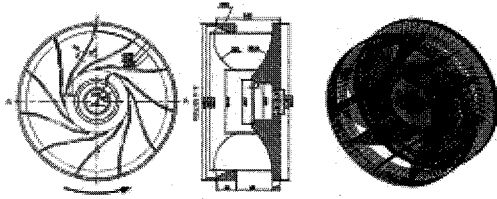


Fig. 1 A schematic drawing of a turbine with guide vanes and flow separation on the suction side of a runner vane

In this process, if flow separation occurs on the vane surface and casing wall (see Fig. 1), it would be a critical reason to degrade the efficiency of the turbine and even to shorten life cycle of the system.

Fig. 2 shows physical and numerical

domain of the model turbine that is incorporated in this numerical and experimental study.



(Physical domain) (Numerical domain)

Fig. 2 Physical and numerical domains of the model Francis hydraulic turbine

3. Numerical scheme and boundary conditions

FVM was employed to simulate airflow phenomenon in the flow path of the model runner. Rotational speed of the runner was fixed with a given head of working fluid. Therefore, blade-to-blade field of the control volume can be reasonably defined as:

- Quasi-3D flow
- Turbulent flow
- Incompressible flow
- Steady state flow

The general-purpose CFD code, PHOENICS (ver.3.1)^[3], was incorporated for a numerical study of the turbulent incompressible flow field. 3-D Navier-Stokes equations were solved with standard (κ - ϵ) turbulent model^[4]. Since the process was assumed as steady state and adiabatic process, and thus the energy equation was not required to solve in the numerical calculation. The turbulent no-slip condition near solid boundary has been modeled by the logarithmic law. Conjugate gradient techniques for pressure corrections in transport equations has

been incorporated and 'SIMPLE' algorithm^[4] has been employed for the velocity and pressure coupling in this application.

3.1 Numerical scheme and boundary conditions

The basic equations of fluid dynamics in the control volume are based on Navier-Stokes equations^[7] that are comprised of equations for conservation of mass and momentum and given as,

Continuity equation

$$\frac{\partial U_i}{\partial x_i} + \frac{\partial U_j}{\partial y_j} + \frac{\partial U_k}{\partial z_k} = 0 \quad (1)$$

Momentum equation

$$\frac{\partial U_i}{\partial t} + \frac{\partial}{\partial x_j} (U_j U_i) = -\frac{1}{\rho} \frac{\partial P}{\partial x_i} + \frac{\partial}{\partial x_j} \left[\nu \left(\frac{\partial U_i}{\partial x_j} + \frac{\partial U_j}{\partial x_i} \right) - \overline{u_i u_j} \right] - g_i \quad (2)$$

Turbulent kinetic equation

$$\frac{\partial}{\partial x_i} (U_j k) = \frac{\partial}{\partial x_i} \left[\left(\nu + \frac{\nu_t}{\sigma_k} \right) \frac{\partial k}{\partial x_j} \right] + G - \epsilon \quad (3)$$

Energy dissipation equation

$$\frac{\partial}{\partial x_i} (U_j \epsilon) = \frac{\partial}{\partial x_i} \left[\left(\nu + \frac{\nu_t}{\sigma_\epsilon} \right) \frac{\partial \epsilon}{\partial x_j} \right] + \frac{\epsilon}{k} (C_{\epsilon 1} G - C_{\epsilon 2} \epsilon) \quad (4)$$

where

$$G = - \overline{u_i u_j} \frac{\partial U_i}{\partial x_j}, \quad \nu_t = C_\mu \frac{k^2}{\epsilon}$$

$$(C_\mu = 0.09, C_{\epsilon 1} = 1.44, C_{\epsilon 2} = 1.92, \sigma_k = 1.0, \sigma_\epsilon = 1.0)$$

3.2 Numerical domain of physical model and its conditions

BFC^[5] grid generation method in conjunction with non-orthogonal grids allowing irregular geometries has been

used to generate the numerical grid and the optimized grid size of the 3-D model was 52x64x12. Fig. 3 shows a prospective 3-D numerical domain of blade-to-blade path of the rotor incorporated for this numerical study.

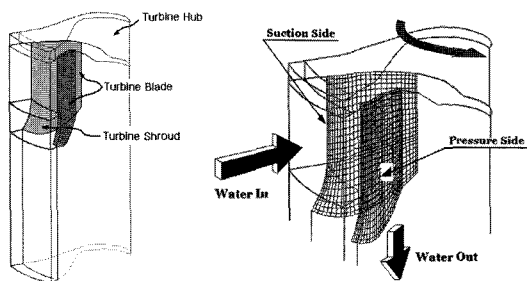


Fig. 3 A prospective view of 3-D numerical domain of blade-to-blade path of the rotor (52x64x12)

Boundary and initial conditions of the calculation:

- (1) Velocity boundary condition at the inlet of the control volume
- (2) Pressure boundary condition at the exit of the control volume
- (3) No-slip condition at the surface of the model impeller: blades, hub, shroud ring
- (4) Symmetric boundary condition on the open surface of the control volume: high and low surface

3.3 Major parameters and their ranges

The output power of the hydraulic turbine is controlled by the mass flowrate of water and its head in a volute. An induced angle at the inlet of the turbine is a critical design parameter of the turbine system. In

this study, the induced angle was controlled by the inlet guide vanes from fully closed position to partly opened position up to 45degree angle by 6 steps to have its effect on the power performance of the turbine system. Fig. 4 shows the top view of the model turbine assembly.

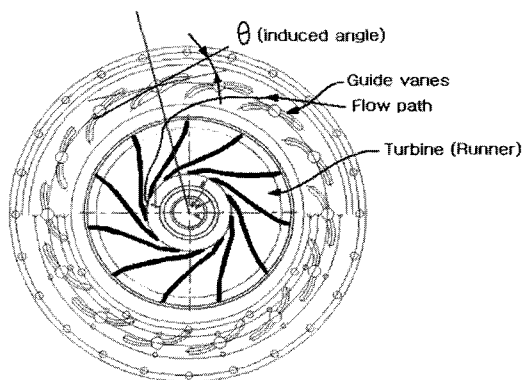


Fig. 4 Top view of the model turbine and its induced angle

Table 1 Experimental output of model turbine supplied by KIER^[6]

Model No.	Induced Angle (degree)	Rotational Speed (rpm)	Head (mAq)	Flowrate (m ³ /s)	Torque (N.m)
Model-25	11.3	617.5	6.5	0.052	13.58
Model-40	18.0	637.0	6.5	0.065	22.85
Model-55	24.8	655.0	5.5	0.089	30.46
Model-70	31.5	669.9	5.0	0.107	34.15
Model-85	40.5	706.3	5.0	0.126	38.91
Model-100	45.0	716.1	5.0	0.140	38.89

Table 1 shows the variation of the induced angle of the turbine set for the experimental study. It also shows some important experimental outputs such as the variation of mass flowrate and rotational speed of the turbine. The

information is incorporated as boundary conditions to this numerical study.

4. Performance analysis of model turbine

From the simulation result, the indicated power of the model turbine can be estimated. The static pressure distribution on the surface of the model impeller is energy source for the torque generated on the turbine shaft. The static pressure force can be calculated from the equations given below^[8].

- (1) Hydrostatic pressure force on the impeller vane:

$$F = \int_A P(x, y) dA \quad (5)$$

- (2) Indicated torque (τ_i) generated on the turbine shaft:

$$\tau_i = \Delta F \times l_{cp} \quad (6)$$

where $\Delta F = F_{pressure} - F_{suction}$

- (3) Indicated power (P_i) produced on the model turbine:

$$P_i = \tau_i \times \omega \quad (7)$$

where ω is rotational speed of the turbine

- (4) Turbine efficiency:

$$\eta_i = \frac{P_i}{P_m} \times 100 \quad (\%) \quad \eta_b = \frac{P_b}{P_m} \times 100 \quad (\%) \quad (8)$$

where η_i : turbine indicated efficiency.

η_{t_b} : turbine brake efficiency

- (5) Mechanical efficiency of the model turbine:

$$\eta_m = \frac{P_b}{P_i} \times 100 \quad (\%) \quad (9)$$

where P_b is brake power measured at the experiment

- (6) Mechanical loss power of the model turbine:

$$P_{loss} = P_i - P_b \quad (10)$$

5. Results and discussion

In this numerical study, mechanical efficiency of the turbine was calculated from the comparison of input power to brake and indicated output power of the turbine. An efficiency of the turbine is very important performance parameter to estimate the energy conversion efficiency of the designed system. The mechanical loss power of the model turbine was also found from the comparison of indicated power to brake power obtained from the experimentation.

Fig. 5 shows the velocity and pressure distribution at the entrance of the impeller. In the case of velocity distribution, water is accelerated at the lower side of the entrance because the fluid turns down its direction into 90 degrees at the entrance. Pressure distribution on the pressure side of the vane is much higher than on the suction side.

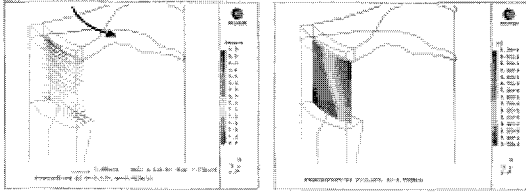


Fig. 5 Velocity and pressure distributions at the entrance of the impeller; induced angle = 11.3 degree

Fig. 6 shows velocity distribution on meridian section at the entrance. As shown, three complex flow zones appear in the flow regions. At the entrance region①, flow direction changes abruptly and very strong vortex is expected that is a sink of flow energy. In the hub region ②, water flows in opposite direction to the rotor and it may also generate the tip vortex as it goes back to the suction side of the vane. The same flow phenomenon happens at the exit of the vane③.

Fig. 7 shows static pressure distributions on the pressure and suction side of the vane. The pressure side of the vane has higher pressure distribution than on the suction side. This is very important information to estimate the indicate power of the designed impeller.

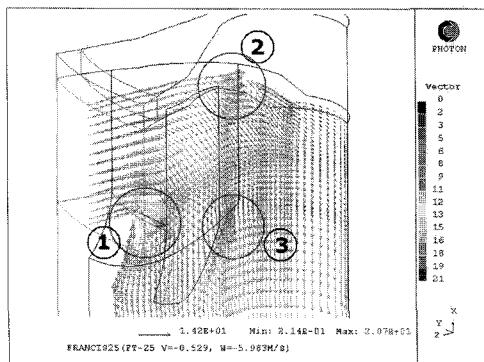
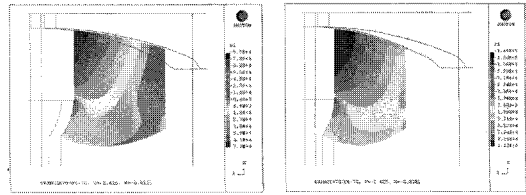


Fig. 6 Velocity distribution at meridian line of the impeller; induced angle = 11.3 degree



(suction-side) (pressure-side)

Fig. 7 Hydrostatic pressure distribution on the pressure and suction surface of the vane of the model turbine at 31.5 degree of induced angle

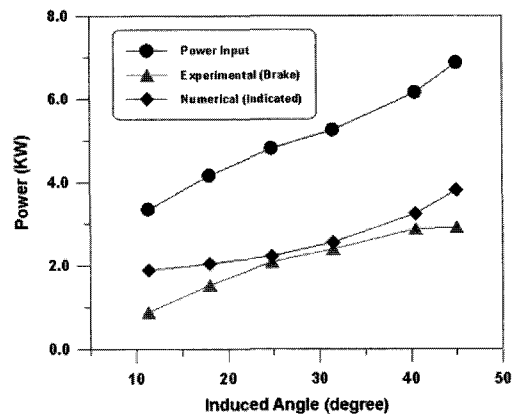
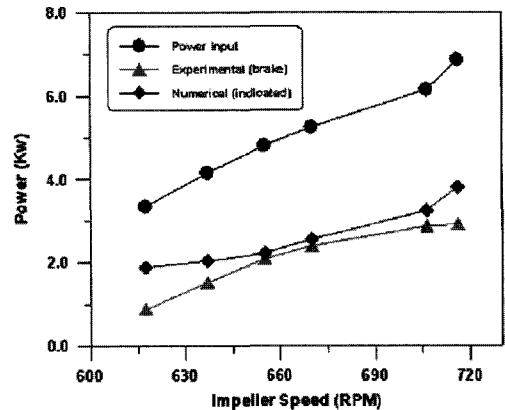


Fig. 8 Variation of power input and output of the model turbine with respect to rotational speed and induced angle

Fig. 8 shows variation of power input and output of the model turbine. The rotational speed of the turbine is directly related to mass flowrate of the inlet water and induced angle as well. As

shown in the figure, all the powers are continuously increasing along with the impeller. Especially the output power difference between brake and indicated power is minimized at the middle range of speed. It means that the mechanical energy loss of the impeller is minimized at the middle speed range.

Fig. 9 shows variation of mechanical efficiency of the turbine with respect to the induced angle. As shown in the figure, mechanical efficiency of the turbine is maximized in the middle range of the induced angle. In general, it is known that the mechanical efficiency of Francis hydraulic turbine is around 85~90%. For the model turbine incorporated in this study, it is estimated that the best operating condition of this model turbine is on 25~30 degree of induced angle and its best efficiency is around 93%. Mean value of the mechanical efficiency of this turbine model is around 79%.

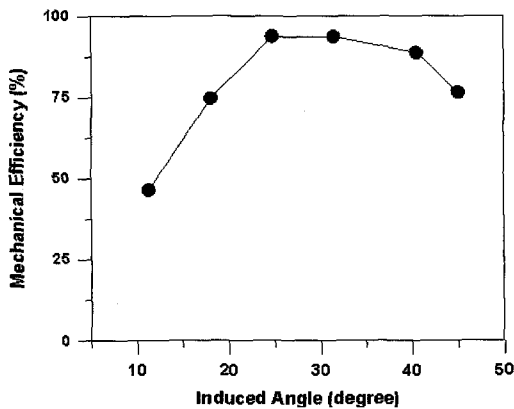


Fig. 9 Variation of mechanical efficiency of the model turbine with respect to induced angle

In Fig. 10, brake and indicated efficiency of the model turbine were compared. The indicated efficiency is minimized in the

middle range of induced angle; however, the brake efficiency is on the other way. For the indicated efficiency, the value is seriously affected by the flow phenomenon in the flow path of the turbine. It means that the flow is quite stable in the lower and higher indicated angle. The brake efficiency is related to mechanical loss of the turbine. As shown in Fig. 11, mechanical loss is minimized in the middle range of the induced angle.

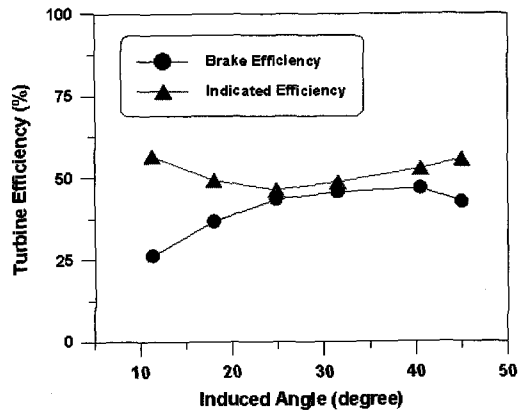


Fig. 10 Variation of brake and indicated efficiency of the model turbine with respect to induced angle

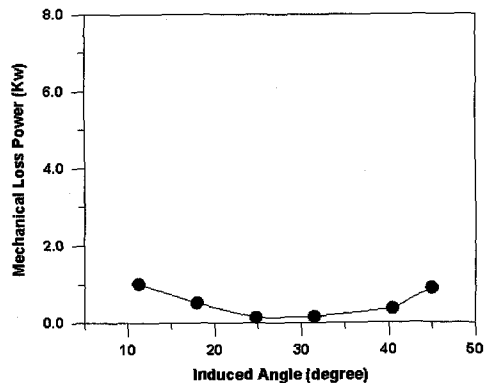


Fig. 11 Variation of mechanical loss power of the model turbine with respect to induced angle

Fig. 11 shows mechanical loss power of the model turbine. The loss power is minimized in the middle range of the induced angle. It means that the optimum operating range of the model turbine is on 25 ~35 degree of induced angle.

6. Conclusion

From this numerical study, it was found that induced angle at the inlet of Francis hydraulic turbine controlled by the inlet guide vane system affects very seriously to the output power generated on the hydraulic turbine; that is, the induced angle is very important parameter for an optimum design of the hydraulic turbine. In this study, the induced angle is the only parameter to control to see its effect on the output power performance of the model turbine. However, mass flowrate and hydraulic head will be studied to have their effects on the general performance of the model turbine.

In the case of this model Francis hydraulic turbine designed by KIERT^[6], the induced angle should be adjusted to 25 to 30 degree at the given hydraulic head and rotational speed to have its best performance in operation.

References

- [1] W. S. Janna, Introduction to Fluid Mechanics, 3rd edition, PWS Publishing Co, pp.512-535, 1993.
- [2] D. G. Shepherd, Principle of Turbomachinery, 4th edition, The Macmillan Co, pp.282-305, 1964.
- [3] PHOENICS PIL Manual, Version 3.1, CHAM Ltd. 2002.
- [4] S. V. Patankar, Numerical Heat Transfer and Fluid Flow, Hemisphere Publishing Corp. 1980.
- [5] R. L. Thompson, Body Fitted Coordinate, John Wiley & Sons, Inc. 1991.
- [6] C. H. Lee and W. S. Park, Development of Francis Type Hydro Turbine for Low & Medium Head, Technical Report, 2004.
- [7] M. Potter and D. Wiggert, Mechanics of Fluids, Brooks/Cole, 3rd edition, p.1-60, 2002.
- [8] Table Curve 2D Manual, V5.0, SPSS Science Co, 2002.

Author Profile



Chul-Ho Kim

He received the B.E and M.E. degree from Inha University in Korea, Ph. D. degree from The University of New South Wales in Sydney. He is currently associate professor at Department of Automotive Engineering, Seoul National University of Technology.

His research interest is aerodynamic design with an application of CFD method.